

A Spectral Boundary Integral Equation Method for the 2D Helmholtz Equation

FANG Q. HU

Department of Mathematics and Statistics, Old Dominion University, Norfolk, Virginia 23529

February 22, 1994; revised September 9, 1994

In this paper, we present a new numerical formulation of solving the boundary integral equations reformulated from the Helmholtz equation. The boundaries of the problems are assumed to be smooth closed contours. The solution on the boundary is treated as a periodic function, which is in turn approximated by a truncated Fourier series. A Fourier collocation method is followed in which the boundary integral equation is transformed into a system of algebraic equations. It is shown that in order to achieve spectral accuracy for the numerical formulation, the non-smoothness of the integral kernels, associated with the Helmholtz equation, must be carefully removed. The emphasis of the paper is on investigating the essential elements of removing the non-smoothness of the integral kernels in the spectral implementation. The present method is robust for a general smooth boundary contour. Aspects of efficient implementation of the method using FFT are also discussed. Numerical examples of wave scattering are given in which the exponential accuracy of the present numerical method is demonstrated. © 1995 Academic Press, Inc.

1. INTRODUCTION

The *boundary integral equation method* is a powerful tool for solving certain boundary value problems. It is particularly attractive in developing numerical methods since, when applied, it reduces the dimension of the problem and often transforms a problem in an infinite domain to integrals on the finite boundary in which the far field radiation condition is satisfied automatically.

Numerical methods for the boundary integral equations have been developed predominantly based on the boundary element method (BEM) [1]. In this method the physical boundary is divided into finite elements and integrations over each element are approximated by numerical quadratures. In this way, the integral equation is converted into a system of algebraic equations. BEM has gone through a rapid advancement in recent years. Its applications to the Helmholtz equation are discussed in Ref. [2] and the references cited therein. Other formulations of solving the boundary integral equations in wave scattering and propagation have also been proposed in the past, including, for example, the T-matrix method [3–5].

In this paper, we present a spectral method formulation for solving the boundary integral equations reformulated from the Helmholtz equation. For the Fourier approximations used in this paper, we assume that the boundary of the problem is a smooth closed contour. The functions appearing in the 2D boundary integral equation will be treated as periodic functions, which are in turn approximated with high accuracy using truncated Fourier series. The boundary integral equation is then transformed into a system of linear algebraic equations. The spectral methods have been known to have extremely fast convergence rates, faster than any finite power of $1/N$ when the solution is infinitely smooth [6, 7] (where N is the number of collocation points). The present numerical formulation will be seen to have spectral accuracy.

It is known that, although any periodic function can be approximated by a truncated Fourier series, the rate of convergence depends on its smoothness. Unfortunately, the integral kernels for the Helmholtz equation are not smooth. In particular, we note that the 2D Green's function, appearing in the integral equations, possesses a logarithmic singularity. Furthermore, the normal derivative of the Green's function also contains a term involving the logarithmic function. It will be seen that it is critical to remove the non-smoothness of the integral kernel in order to achieve fast convergence in the spectral formulation. In this paper the non-smoothness of the integral kernels is subtracted out by using a logarithmic periodic function whose Fourier expansion is known.

Fourier approximation methods for the boundary integral equations in wave scattering have been proposed in the past for simple geometries. A "fast numerical method" has been formulated by Bojarski [8] for wave scattering by a circular cylinder. It was pointed out that the boundary integral equation for scattering by a hard circular cylinder can be solved easily and efficiently in the Fourier spectrum domain of the solution. Due to the special geometry considered, a simple relation for the Fourier coefficients of the solution and those of the boundary condition was derived. Recently a similar numerical approach has been applied by Schuster [9] for a wave transmission problem of concentric cylinders. However, in these works the singularities and non-smoothness of the integral kernels were not

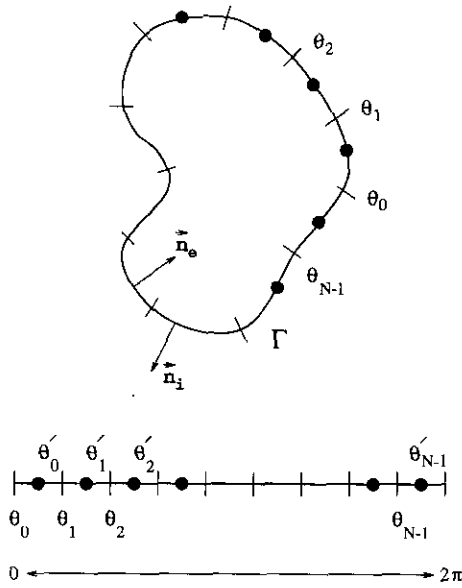


FIG. 1. Schematic of discretization of the boundary. θ is the parameterizing variable for the boundary contour. \mathbf{n}_e and \mathbf{n}_i indicate the direction of the normal vector for an exterior and interior problem respectively.

removed. Consequently the convergence rates of these methods were not exponential.

In Section 2, a formulation of the boundary integral equation for the Helmholtz equation is given, followed by a discretization using a Fourier collocation method. Essential elements of achieving spectral accuracy are investigated. In Section 3, a numerical example is given in which the spectral rate of convergence is demonstrated. Section 4 contains the conclusions.

2. FORMULATIONS

2.1. Boundary Integral Equations

Consider wave propagation in an interior or exterior domain with a smooth closed boundary Γ (Fig. 1). The wave equation for a scalar function ϕ with assumed time dependency of $e^{-i\omega t}$ is reduced to the Helmholtz equation

$$\nabla^2 \phi + \kappa^2 \phi = 0, \quad (1)$$

where κ is the wave number and ∇^2 is the 2D Laplace operator, $\nabla^2 = \partial^2/\partial x^2 + \partial^2/\partial y^2$. The boundary condition considered in this paper is one of the following types:

Dirichlet: $\phi(\mathbf{r}) = a(\mathbf{r})$ on Γ

Neumann: $(\partial\phi/\partial n)(\mathbf{r}) = b(\mathbf{r})$ on Γ

Robin (impedance): $\alpha\phi(\mathbf{r}) + \beta(\partial\phi/\partial n)(\mathbf{r}) = c(\mathbf{r})$ on Γ .

The Helmholtz equation (1) can be reformulated into a boundary integral equation in various ways [10, 11]. Our pur-

pose in this paper is to demonstrate the spectral approximations and the essential elements of achieving spectral accuracy. A *direct* formulation of the boundary integral equation employing the Green's function will be used here which leads to an integral equation involving ϕ and its normal derivative on the boundary [2]:

$$\frac{1}{2} \phi(\mathbf{r}') + \int_{\Gamma} \phi \frac{\partial G}{\partial n} d\Gamma = \int_{\Gamma} G \frac{\partial \phi}{\partial n} d\Gamma, \quad (2)$$

where $\partial/\partial n$ denotes the normal derivative, with the direction of \mathbf{n} being outward from the domain of wave propagation, and \mathbf{r}' denotes a point on the boundary. The Green's function $G(\mathbf{r}, \mathbf{r}')$, whose form will be given later, satisfies the equation

$$\nabla^2 G + \kappa^2 G = -\delta(\mathbf{r} - \mathbf{r}'). \quad (3)$$

Once the values of ϕ and $\partial\phi/\partial n$ on the boundary are found, the solution at any point, \mathbf{r} , inside the domain of wave propagation can be obtained as [2]

$$\phi(\mathbf{r}) = \int_{\Gamma} \left(G \frac{\partial \phi}{\partial n} - \phi \frac{\partial G}{\partial n} \right) d\Gamma.$$

Without loss of generality, let us now assume that the boundary curve Γ is parameterized as

$$\mathbf{r}_{\Gamma} = \mathbf{r}(\theta), \quad 0 \leq \theta \leq 2\pi, \quad (4)$$

where θ is a non-dimensional parameter for the boundary contour, not necessarily the arclength or some angle. In addition, the curve is supposed to be simple, that is,

$$\left| \frac{d\mathbf{r}}{d\theta} \right| = \sqrt{(dx/d\theta)^2 + (dy/d\theta)^2} \neq 0.$$

For simplicity, we further assume that $\mathbf{r}(\theta)$ is infinitely differentiable. Then the boundary integral equation (2) can be written as

$$\begin{aligned} \frac{1}{2} \phi(\theta') + \int_0^{2\pi} \phi(\theta) \frac{\partial G}{\partial n}(\theta, \theta') \left| \frac{d\mathbf{r}}{d\theta} \right| d\theta \\ = \int_0^{2\pi} \frac{\partial \phi}{\partial n}(\theta) G(\theta, \theta') \left| \frac{d\mathbf{r}}{d\theta} \right| d\theta \end{aligned} \quad (5)$$

in which the line element $d\Gamma = |d\mathbf{r}/d\theta| d\theta$. For clarity, the dependencies on θ and θ' have been expressed explicitly in (5).

For the 2D Helmholtz equation, the outgoing Green's function and its normal derivative are [12]

$$G(\theta, \theta') = (i/4) H_0^{(3)}(\kappa R) \quad (6)$$

$$\frac{\partial G}{\partial \mathbf{n}}(\theta, \theta') = -\frac{i\kappa}{4} H_1^{(1)}(\kappa R) \frac{\mathbf{R} \cdot \mathbf{n}}{R} \quad (7)$$

in which we have used the notations that $\mathbf{R} = \mathbf{r}(\theta) - \mathbf{r}(\theta')$ and $R = |\mathbf{R}|$. Here $H_0^{(1)}$ and $H_1^{(1)}$ are respectively the first kind Hankel functions of order zero and one.

2.2. Spectral Approximations

For a closed boundary Γ , $\phi(\theta)$ and $(\partial\phi/\partial n)(\theta)$ are periodic functions of θ , for $0 \leq \theta \leq 2\pi$. Let ϕ and $\partial\phi/\partial n$ be approximated by truncated Fourier series as

$$\phi^N(\theta) = \sum_{n=-N/2}^{N/2-1} \hat{\phi}_n e^{in\theta} \quad (8)$$

$$\frac{\partial \phi^N}{\partial n}(\theta) = \sum_{n=-N/2}^{N/2-1} \hat{\psi}_n e^{in\theta}. \quad (9)$$

The particular form of the truncated Fourier series has been taken in (8) and (9) for the convenience of using discrete fast Fourier transform (FFT) programs [7]. Substituting (8) and (9) into (5), the boundary integral equation becomes

$$\begin{aligned} & \frac{1}{2} \sum_{n=-N/2}^{N/2-1} \hat{\phi}_n e^{in\theta'} + \sum_{n=-N/2}^{N/2-1} \hat{\phi}_n \int_0^{2\pi} e^{in\theta} \frac{\partial G}{\partial n}(\theta, \theta') \left| \frac{d\mathbf{r}}{d\theta} \right| d\theta \\ & = \sum_{n=-N/2}^{N/2-1} \hat{\psi}_n \int_0^{2\pi} e^{in\theta} G(\theta, \theta') \left| \frac{d\mathbf{r}}{d\theta} \right| d\theta. \end{aligned} \quad (10)$$

We note that the two integrals in (10) are actually the Fourier coefficients of $G(\theta, \theta') |d\mathbf{r}/d\theta|$ and $\partial G/\partial n(\theta, \theta') |d\mathbf{r}/d\theta|$, respectively. Our aim is to evaluate the integrals by the fast Fourier transforms with spectral accuracy.

It is clear that both $G(\theta, \theta') |d\mathbf{r}/d\theta|$ and $(\partial G/\partial n)(\theta, \theta') |d\mathbf{r}/d\theta|$ are periodic functions of θ and θ' . They are also infinitely differentiable except at $\theta = \theta'$, where $R = 0$ in (6) and (7). Although any periodic function can be approximated in a truncated Fourier series, the rate of convergence depends on the smoothness of the function. From this consideration, we note that, first, $G(\theta, \theta')$ has a logarithmic singularity at $R = 0$, due to the Hankel function of order zero in (6). Second, although $(\partial G/\partial n)(\theta, \theta')$ can be shown to be a finite function, it is not infinitely smooth. It is easy to show that the function R has a discontinuous derivative at $\theta = \theta'$. In particular, for $|\theta - \theta'|$ small, we have

$$\begin{aligned} R = |\mathbf{r}(\theta) - \mathbf{r}(\theta')| &= \left| \frac{d\mathbf{r}}{d\theta} \cdot (\theta - \theta') + \frac{1}{2} \frac{d^2\mathbf{r}}{d\theta^2} \cdot (\theta - \theta')^2 + \dots \right| \\ &= |\theta - \theta'| \left| \frac{d\mathbf{r}}{d\theta} + \frac{1}{2} \frac{d^2\mathbf{r}}{d\theta^2} (\theta - \theta') + \dots \right|. \end{aligned} \quad (11)$$

Consequently any term with an odd power or logarithmic func-

tion of R will not be infinitely smooth and has to be treated in order to achieve spectral accuracy in the Fourier approximation.

To study the singularity in $G(\theta, \theta')$, we note that

$$G(\theta, \theta') = \frac{i}{4} H_0^{(1)}(\kappa R) = \frac{i}{4} (J_0(\kappa R) + iY_0(\kappa R))$$

in which J_0 and Y_0 are zeroth order Bessel functions of the first and second kind, respectively. Using the asymptotic series for a small argument [13],

$$J_0(\kappa R) = 1 - \frac{(\kappa R)^2}{4} + \frac{(\kappa R)^4}{64} - \dots$$

$$Y_0(\kappa R) = \frac{2}{\pi} \ln\left(\frac{\kappa R}{2}\right) J_0(\kappa R) + \frac{2\gamma}{\pi} J_0(\kappa R) + \frac{(\kappa R)^2}{2\pi} - \dots,$$

we have, for $|\theta - \theta'|$ small,

$$\begin{aligned} G(\theta, \theta') &= \frac{i}{4} (J_0(\kappa R) + iY_0(\kappa R)) \\ &= -\frac{1}{2\pi} \ln\left(\frac{\kappa R}{2}\right) J_0(\kappa R) + (\text{smooth terms}) \end{aligned}$$

in which ‘‘smooth terms’’ represents a convergent power series containing only the even powers of R , and J_0 is the regular Bessel function of zeroth order which is also a power series of R^2 [13]. To remove the logarithmic singularity but preserve the periodicity, consider the *periodic* function $\ln |2 \sin((\theta - \theta')/2)|$, which has a logarithmic singularity at $\theta = \theta'$. Its Fourier series can be found exactly [12]:

$$\ln \left| 2 \sin\left(\frac{\theta - \theta'}{2}\right) \right| = -\sum_{n=1}^{\infty} \frac{\cos n(\theta - \theta')}{n}. \quad (12)$$

To subtract out the singularity in $G(\theta, \theta')$, let

$$\bar{G}(\theta, \theta') \equiv \frac{i}{4} H_0^{(1)}(\kappa R) + \frac{1}{2\pi} \ln \left| 2 \sin\left(\frac{\theta - \theta'}{2}\right) \right| J_0(\kappa R).$$

Then the Green’s function is found as

$$G(\theta, \theta') = \bar{G}(\theta, \theta') - \frac{1}{2\pi} \ln \left| 2 \sin\left(\frac{\theta - \theta'}{2}\right) \right| J_0(\kappa R). \quad (13)$$

Using (11), it is easy to show that $\bar{G}(\theta, \theta')$ is periodic but finite for all values of the arguments. Furthermore, both $\bar{G}(\theta, \theta')$ and $J_0(\kappa R)$ are now infinitely differentiable functions. Thus the Fourier coefficients of $G(\theta, \theta') |d\mathbf{r}/d\theta|$ can be computed according to (13) with spectral accuracy. For the term involving the logarithmic function in (13), convolution sums will be used.

We now study the singularities in the normal derivative of the Green's function $\partial G/\partial n$. The asymptotic expression of $H_1^{(1)}(\kappa R)$ for κR small has the following form [13]

$$\begin{aligned} H_1^{(1)}(\kappa R) &= J_1(\kappa R) + iY_1(\kappa R) \\ &= J_1(\kappa R) + i \left(-\frac{2}{\pi \kappa R} + \frac{2}{\pi} \ln \left(\frac{\kappa R}{2} \right) J_1(\kappa R) \right. \\ &\quad \left. + \text{odd powers of } \kappa R \right) \\ &= -\frac{2i}{\pi \kappa R} + \frac{2i}{\pi} \ln \left(\frac{\kappa R}{2} \right) J_1(\kappa R) + \text{odd powers of } \kappa R \end{aligned}$$

in which we have used the fact that the Bessel function of order unity, J_1 , is a power series of odd power of κR ,

$$J_1(\kappa R) = \frac{\kappa R}{2} - \frac{(\kappa R)^3}{16} + \dots$$

In addition, it can be shown that $\mathbf{R} \cdot \mathbf{n} = O((\theta - \theta')^2)$. Thus it follows that

$$\begin{aligned} \frac{\partial G}{\partial n}(\theta, \theta') &= -\frac{i\kappa}{4} \left(-\frac{2i}{\pi \kappa R} + \frac{2i}{\pi} \ln \left(\frac{\kappa R}{2} \right) J_1(\kappa R) \right. \\ &\quad \left. + \text{odd powers of } \kappa R \right) \frac{\mathbf{R} \cdot \mathbf{n}}{R} \\ &= \frac{\kappa}{2\pi} \ln \left(\frac{\kappa R}{2} \right) J_1(\kappa R) \frac{\mathbf{R} \cdot \mathbf{n}}{R} + (\text{smooth terms}). \end{aligned}$$

It is seen that, although $\partial G/\partial n$ is a finite function, it does not have smooth derivatives due to the logarithmic function that appeared in the first term shown above. For this reason, its Fourier approximation will converge only at a finite rate of $1/N^3$. To smooth out the function for computations by FFT, let

$$\begin{aligned} \bar{H}(\theta, \theta') &= -\frac{i\kappa}{4} H_1^{(1)}(\kappa R) \frac{\mathbf{R} \cdot \mathbf{n}}{R} \\ &\quad - \frac{\kappa}{2\pi} \ln \left| 2 \sin \left(\frac{\theta - \theta'}{2} \right) \right| J_1(\kappa R) \frac{\mathbf{R} \cdot \mathbf{n}}{R}. \end{aligned}$$

Then

$$\begin{aligned} \frac{\partial G}{\partial n}(\theta, \theta') &= \bar{H}(\theta, \theta') \\ &\quad + \frac{\kappa}{2\pi} \ln \left| 2 \sin \left(\frac{\theta - \theta'}{2} \right) \right| J_1(\kappa R) \frac{\mathbf{R} \cdot \mathbf{n}}{R}. \end{aligned} \quad (14)$$

The functions $\bar{H}(\theta, \theta')$ and $J_1(\kappa R) (\mathbf{R} \cdot \mathbf{n}/R)$ in (14) are now

periodic and infinitely differentiable. The Fourier coefficients of $(\partial G/\partial n)(\theta, \theta') |d\mathbf{r}/d\theta|$ will be computed according to (14).

Following the above analysis, we then express the boundary integral equation (10) as

$$\begin{aligned} \frac{1}{2} \sum_{n=-N/2}^{N/2-1} \hat{\phi}_n e^{in\theta'} + \sum_{n=-N/2}^{N/2-1} \hat{\phi}_n \left(\int_0^{2\pi} e^{in\theta} \bar{H}(\theta, \theta') \left| \frac{d\mathbf{r}}{d\theta} \right| d\theta \right. \\ \left. + \frac{\kappa}{2\pi} \int_0^{2\pi} e^{in\theta} \ln \left| 2 \sin \left(\frac{\theta - \theta'}{2} \right) \right| J_1(\kappa R) \frac{\mathbf{R} \cdot \mathbf{n}}{R} \left| \frac{d\mathbf{r}}{d\theta} \right| d\theta \right) \\ = \sum_{n=-N/2}^{N/2-1} \hat{\psi}_n \left(\int_0^{2\pi} e^{in\theta} \bar{G}(\theta, \theta') \left| \frac{d\mathbf{r}}{d\theta} \right| d\theta \right. \\ \left. - \frac{1}{2\pi} \int_0^{2\pi} e^{in\theta} \ln \left| 2 \sin \left(\frac{\theta - \theta'}{2} \right) \right| J_0(\kappa R) \left| \frac{d\mathbf{r}}{d\theta} \right| d\theta \right). \end{aligned} \quad (15)$$

Now all the integrals in (15) are in a form which can be evaluated numerically with spectral accuracy.

2.3. Discretization

In what follows, a spectral collocation approach will be taken in deriving the algebraic system for the boundary integral equation (15). Let us introduce two sets of discretization points (Fig. 1)

$$\begin{aligned} \theta_j &= 2\pi j/N, & j &= 0, 1, \dots, N-1, \\ \theta'_j &= 2\pi(j + \frac{1}{2})/N, & j' &= 0, 1, \dots, N-1. \end{aligned}$$

The reason for using two sets of discretization points, as will be clear later, is that it avoids the direct evaluations of $\bar{G}(\theta, \theta')$ and $\bar{H}(\theta, \theta')$ at points where $\theta = \theta'$. Although both functions are finite there, their limits are geometry dependent. The current discretization is robust. We then require that the boundary integral equation (15) be satisfied at collocation points $\theta' = \theta'_j, j' = 0, 1, \dots, N-1$.

For convenience of discussion, we denote the following Fourier series approximations at θ'_j for $j' = 0, 1, \dots, N-1$,

$$\bar{G}(\theta, \theta'_j) \left| \frac{d\mathbf{r}}{d\theta} \right| = \sum_{n=-N/2}^{N/2-1} g_{j'n} e^{-in\theta} \quad (16a)$$

$$\bar{H}(\theta, \theta'_j) \left| \frac{d\mathbf{r}}{d\theta} \right| = \sum_{n=-N/2}^{N/2-1} h_{j'n} e^{-in\theta} \quad (16b)$$

$$[J_0(\kappa R)]_{\theta'_j} \left| \frac{d\mathbf{r}}{d\theta} \right| = \sum_{n=-N/2}^{N/2-1} p_{j'n} e^{-in\theta} \quad (16c)$$

$$\left[J_1(\kappa R) \frac{\mathbf{R} \cdot \mathbf{n}}{R} \right]_{\theta'_j} \left| \frac{d\mathbf{r}}{d\theta} \right| = \sum_{n=-N/2}^{N/2-1} q_{j'n} e^{-in\theta}. \quad (16d)$$

The coefficients of the expansions are calculated by FFT (backward in the usual sense) as

$$g_{j'n} = \frac{1}{N} \sum_{j=0}^{N-1} e^{in\theta_j} \overline{G}(\theta_j, \theta'_j) \left| \frac{d\mathbf{r}}{d\theta}(\theta_j) \right| \quad (16a')$$

$$h_{j'n} = \frac{1}{N} \sum_{j=0}^{N-1} e^{in\theta_j} \overline{H}(\theta_j, \theta'_j) \left| \frac{d\mathbf{r}}{d\theta}(\theta_j) \right| \quad (16b')$$

$$p_{j'n} = \frac{1}{N} \sum_{j=0}^{N-1} e^{in\theta_j} [J_0(\kappa R)]_{\theta'_j} \left| \frac{d\mathbf{r}}{d\theta}(\theta_j) \right| \quad (16c')$$

$$q_{j'n} = \frac{1}{N} \sum_{j=0}^{N-1} e^{in\theta_j} \left[J_1(\kappa R) \frac{\mathbf{R} \cdot \mathbf{r}}{R} \right]_{\theta'_j} \left| \frac{d\mathbf{r}}{d\theta}(\theta_j) \right|. \quad (16d')$$

In addition, we denote (12) as

$$\ln \left| 2 \sin \left(\frac{\theta - \theta'}{2} \right) \right| = \sum_{n=-\infty}^{\infty} a_n e^{-in(\theta - \theta')}, \quad (16e)$$

where $a_0 = 0$ and $a_n = -1/2|n|$ for $n \neq 0$.

It is immediately seen that the two integrals involving \overline{G} and \overline{H} in (15) equal $2\pi g_{j'n}$ and $2\pi h_{j'n}$, respectively. The other two integrals are obtainable by convolution sums. Specifically, using the definitions given in (16), we have

$$\begin{aligned} u_{j'n} &= \frac{1}{2\pi} \int_0^{2\pi} e^{in\theta} \ln \left| 2 \sin \left(\frac{\theta - \theta'_j}{2} \right) \right| J_0(\kappa R) \left| \frac{d\mathbf{r}}{d\theta} \right| d\theta \\ &= \sum_{m=-N/2}^{N/2-1} p_{j'm} a_{n-m} e^{i(n-m)\theta'_j} \end{aligned} \quad (17a)$$

$$\begin{aligned} v_{j'n} &= \frac{1}{2\pi} \int_0^{2\pi} e^{in\theta} \ln \left| 2 \sin \left(\frac{\theta - \theta'_j}{2} \right) \right| J_1(\kappa R) \frac{\mathbf{R} \cdot \mathbf{n}}{R} \left| \frac{d\mathbf{r}}{d\theta} \right| d\theta \\ &= \sum_{m=-N/2}^{N/2-1} q_{j'm} a_{n-m} e^{i(n-m)\theta'_j}. \end{aligned} \quad (17b)$$

By substituting (16) and (17) into (15), the resulting algebraic system is

$$\begin{aligned} \frac{1}{2} \sum_{n=-N/2}^{N/2-1} \hat{\phi}_n e^{in\theta'_j} + \sum_{n=-N/2}^{N/2-1} \hat{\phi}_n (2\pi h_{j'n} + \kappa u_{j'n}) \\ = \sum_{n=-N/2}^{N/2-1} \hat{\psi}_n (2\pi g_{j'n} - v_{j'n}) \end{aligned} \quad (18)$$

for $j' = 0, 1, 2, \dots, N - 1$.

Equation (18) is easily cast into a matrix form

$$A\hat{\Phi} = B\hat{\Psi}, \quad (19)$$

where $\hat{\Phi}$ and $\hat{\Psi}$ are the vectors containing $\hat{\phi}_n$ and $\hat{\psi}_n$, respectively. For Dirichlet boundary condition, $\hat{\Psi}$ is solved from (19) with $\hat{\Phi}$ obtained from the boundary condition and vice versa for

the Neumann boundary conditions. The Robin type impedance boundary condition can be treated similarly.

2.4. Evaluation of Convolution Sums

The convolution sums in (17) require $O(N)$ multiplications for each $u_{j'n}$ and $v_{j'n}$. Thus the total operations of obtaining the convolution sums are of order $O(N^3)$. This cost can be reduced considerably to $O(N^2 \log_2 N)$ by the use of a pseudospectral transformation method with *de-aliasing* techniques [6, 7]. For completeness, the evaluation of (17) with a ‘padding’ de-aliasing technique is given below.

Let $M \geq 3N$ and

$$\xi_j = 2\pi j/M, \quad j = 0, 1, 2, \dots, M - 1.$$

Compute the following using FFT for $j = 0, 1, 2, \dots, M - 1$,

$$\begin{aligned} A_{jj} &= \sum_{m=-M/2}^{M/2-1} \tilde{a}_m e^{im\theta'_j} e^{-im\xi_j} \\ P_{jj} &= \sum_{m=-M/2}^{M/2-1} \tilde{p}_{j'm} e^{im\theta'_j} e^{-im\xi_j}, \end{aligned}$$

where

$$\tilde{a}_m = \begin{cases} a_m, & -N \leq m \leq N - 1, \\ 0, & \text{other,} \end{cases}$$

$$\tilde{p}_{j'm} = \begin{cases} p_{j'm}, & -N/2 \leq m \leq N/2 - 1, \\ 0, & \text{other,} \end{cases}$$

and form the product

$$U_{jj} = A_{jj} P_{jj}.$$

Then the convolution sum $u_{j'n}$ is the (backward) FFT of U_{jj} :

$$u_{j'n} = \frac{1}{M} \sum_{j=0}^{M-1} U_{jj} e^{in\xi_j}$$

for $-N/2 \leq n \leq N/2 - 1$. The convolution sum $v_{j'n}$ can be obtained identically.

3. NUMERICAL EXAMPLE: SCATTERING OF A PLANE WAVE BY AN ELLIPTIC CYLINDER

The numerical method described in the previous section will now be applied to the problem of a plane wave scattering by an elliptic cylinder. Exact solutions of wave scattering by an elliptic cylinder can be easily obtained in infinite series [12]. However, numerical evaluation of the exact infinite series is

TABLE I

Values of $\partial\phi/\partial n$ for the Dirichlet Boundary Condition at Selected Points on the Boundary

N	$\theta = 0^\circ$	$\theta = 90^\circ$	$\theta = 180^\circ$	Relative error
$\kappa = 2\pi$				
32	6.178009567	2.376671291	7.134225119	0.04
48	6.379285016	2.175324633	6.914464114	0.2×10^{-4}
64	6.379334010	2.175259123	6.914387795	0.1×10^{-7}
80	6.379333962	2.175259114	6.914387773	10^{-9}
96	6.379333961	2.175259114	6.914387772	10^{-11}
256	6.379333961	2.175259114	6.914387772	—
$\kappa = 20\pi$				
296	62.830835900	9.8054016493	62.926987291	0.2×10^{-3}
316	62.831401053	9.8048411925	62.926435089	0.1×10^{-5}
336	62.831400190	9.8048403329	62.926435958	10^{-9}
356	62.831400191	9.8048403325	62.926435957	10^{-12}
512	62.831400191	9.8048403325	62.926435957	—

Note. The boundary is given by (20). $a = 2$, $b = 1$, incident angle $\alpha = 0^\circ$.

not easily obtainable due to the complexity of the Mathieu functions involved. Our purpose here is to demonstrate the exponential rate of convergence of the spectral method formulated in the previous section. The numerical results will also be compared with some asymptotic values available in the literature [14].

3.1. Spectral Rate of Convergence

Let the plane incident wave having an incident angle α about the x axis be

$$\phi_i = e^{ik(x \cos \alpha + y \sin \alpha)}.$$

The scattered wave, ϕ , satisfies the Helmholtz equation (1). The boundary conditions considered here are the Dirichlet (soft) type $\phi = -\phi_i$ or the Neumann (hard) type, $\partial\phi/\partial n = -\partial\phi_i/\partial n$.

A simple parameterization of the elliptic cylinder is given by

$$\Gamma: (x, y) = (a \cos \theta, b \sin \theta), \quad 0 \leq \theta \leq 2\pi, \quad (20)$$

where a and b are the major and minor axis of the ellipse. The normal vector on Γ is $\mathbf{n} = -(b \cos \theta, a \sin \theta) / \sqrt{b^2 \cos^2 \theta + a^2 \sin^2 \theta}$.

Numerical results for the Dirichlet boundary condition will be presented first. For this calculation the parameters have been taken to be $a = 2$ and $b = 1$. Two cases are presented with wave numbers $\kappa = 2\pi$ and $\kappa = 20\pi$. In Table I, the values of the solution at three selected points on the boundary are given as the number of collocation points increases. Listed are the values of $|\partial\phi/\partial n|$ at $\theta = 0^\circ, 90^\circ$, and 180° on the boundary for the incident angle $\alpha = 0$. Since no exact value is available, the numerical solutions are compared with the results obtained

TABLE II

Values of $\partial\phi/\partial n$ for the Dirichlet Boundary Condition at Selected Points on the Boundary

N	$\theta = 0^\circ$	$\theta = 90^\circ$	$\theta = 180^\circ$	Relative error
$\kappa = 2\pi$				
32	6.402635098	2.165098187	6.899520927	0.005
48	6.379355527	2.175263759	6.914393819	0.3×10^{-5}
64	6.379334276	2.175259159	6.914387893	0.5×10^{-7}
80	6.379333966	2.175259114	6.914387774	0.5×10^{-9}
96	6.379333961	2.175259114	6.914387772	10^{-11}
256	6.379333961	2.175259114	6.914387772	—
$\kappa = 20\pi$				
236	64.329776062	10.626283399	61.739047992	0.1
256	62.832024705	9.804276790	62.925828886	0.1×10^{-2}
276	62.831400247	9.804840394	62.926435874	0.3×10^{-6}
296	62.831400191	9.804840332	62.926435957	10^{-12}
512	62.831400191	9.804840332	62.926435957	—

Note. The boundary is given by (21). $a = 2$, $b = 1$, incident angle $\alpha = 0^\circ$.

for $N = 256$ and $N = 512$ for the two cases, respectively. Clearly exponential rate of convergence is observed.

We point out that, although the parameterization of the ellipse given in (20) is a convenient one, it may not be the best. For example, the following form of parameterization, which has more uniformly distributed collocation points than (20),

$$\Gamma: (x, y) = (a \cos(\theta + 0.05 \sin(2\theta)), b \sin(\theta + 0.05 \sin(2\theta))), \quad 0 \leq \theta \leq 2\pi, \quad (21)$$

yields the values shown in Table II. A somewhat better accuracy is observed.

In Fig. 2 the solution, $\partial\phi/\partial n$, as a function of θ on the surface of the elliptic cylinder has been plotted. Shown are the results for the number of collocation points being 32 and 256, $\kappa = 2\pi$.

3.2. Far Field Directivity

Far field scattered intensities, computed as $r\phi^2$, have also been calculated. The values on an exterior point are obtained through the boundary integral as

$$\begin{aligned} \phi(\mathbf{r}) &= \int_{\Gamma} \left(G \frac{\partial\phi}{\partial n} - \phi \frac{\partial G}{\partial n} \right) d\Gamma \\ &= \sum_{n=-N/2}^{N/2-1} \hat{\psi}_n \int_0^{2\pi} e^{in\theta} G \left| \frac{d\mathbf{r}}{d\theta} \right| d\theta \\ &\quad - \sum_{n=-N/2}^{N/2-1} \hat{\phi}_n \int_0^{2\pi} e^{in\theta} \frac{\partial G}{\partial n} \left| \frac{d\mathbf{r}}{d\theta} \right| d\theta. \end{aligned} \quad (22)$$

The Green's function for points lying outside of the boundary does not have any singularity. Thus (22) is evaluated using

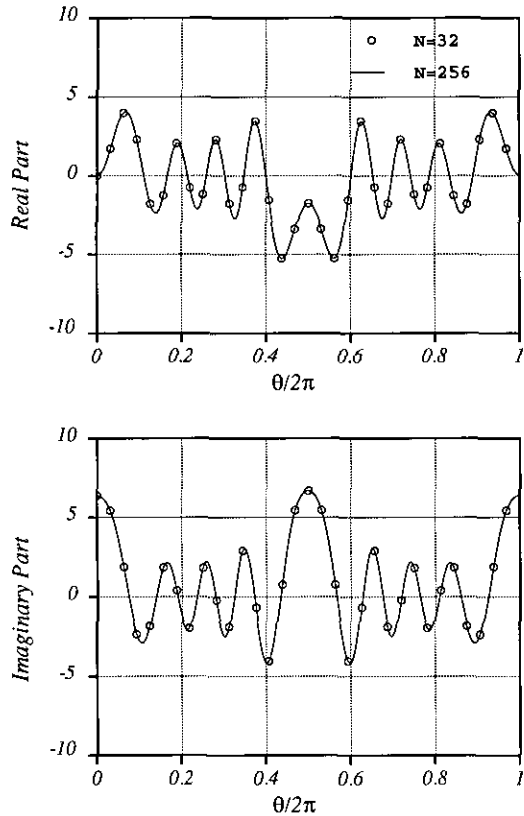


FIG. 2. Solution $\partial\phi/\partial n$ on the surface of the ellipse for the Dirichlet boundary condition. $a = 2$, $b = 1$, and $\kappa = 2\pi$. Plane wave incident angle $\alpha = 0^\circ$. The parameterization of the ellipse is that of (21).

FFT directly. The directivities of the scattered intensity for wave incident angle $\alpha = 0^\circ, 30^\circ, 60^\circ$, and 90° are shown in Fig. 3. For this calculation, $a = 2$, $b = 1$, and $\kappa = 2\pi$.

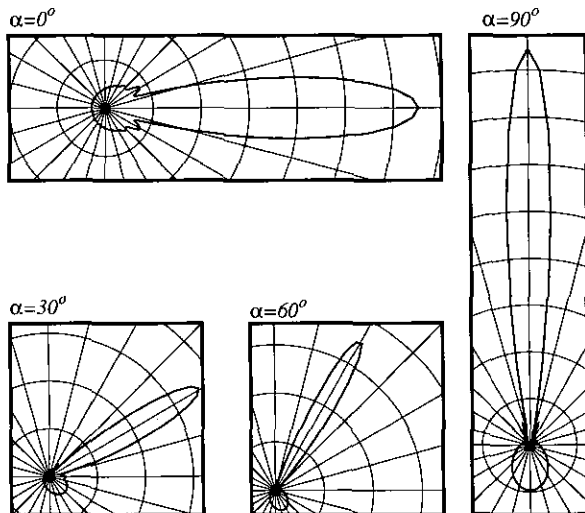


FIG. 3. Far field directives of the scattered wave for indicated incident angles. $a = 2$, $b = 1$, and $\kappa = 2\pi$, with Dirichlet boundary condition.

TABLE III

Values of $r\phi^2$ at Far Field for the Selected Angles

Far field angle	Numerical	Asymptotic [14]
$\mu_0 = 1.0, \theta = 0^\circ, 180^\circ$	1.769057417	1.774
$\mu_0 = 1.0, \theta = 90^\circ$	2.137413140	2.113
$\mu_0 = 1.0, \theta = 270^\circ$	1.538098511	1.491
$\mu_0 = 0.6, \theta = 0^\circ, 180^\circ$	1.364415306	1.367
$\mu_0 = 0.6, \theta = 90^\circ$	1.506576730	1.484
$\mu_0 = 0.6, \theta = 270^\circ$	1.287260683	1.258
$\mu_0 = 0.2, \theta = 0^\circ, 180^\circ$	1.062775602	1.064
$\mu_0 = 0.2, \theta = 90^\circ$	1.107062467	1.087
$\mu_0 = 0.2, \theta = 270^\circ$	1.062022484	1.041

Note. Dirichlet type soft wall boundary conditions are applied. $a = \cosh \mu_0$, $b = \sinh \mu_0$, $\kappa = 0.2$, and incident angle $\alpha = 90^\circ$.

Barakat [14] gives some asymptotic values of long wave scattering of an elliptic cylinder at far field for normal incidence. A comparison of the current numerical results with the asymptotic values is presented in Tables III and IV. For these cases, $a = \cosh \mu_0$, $b = \sinh \mu_0$, and $\kappa = 0.2$. Here μ_0 corresponds to a value in the elliptic coordinates. The results of the far field scattered intensity for $\mu_0 = 1.0, 0.6$, and 0.2 are presented in Tables III and IV for the Dirichlet and Neumann boundary conditions, respectively. For the present long wave scattering, $N = 64$ has been used for all the calculations. The numerical computation agrees with the asymptotic estimation.

Finally, we note that although the exterior scattering problem is uniquely determined, the *direct* formulation of the boundary integral equation used here would not yield a unique solution when the wave number κ coincides with the eigenvalues of a correspondent interior homogeneous problem. On the other hand, this numerical difficulty is well understood and remedies are readily available [10, 11]. For example, unique solution

TABLE IV

Values of $r\phi^2$ at Far Field for the Selected Angles

Far field angle	Numerical	Asymptotic [14]
$\mu_0 = 1.0, \theta = 0^\circ, 180^\circ$	0.009175011010	0.00884
$\mu_0 = 1.0, \theta = 90^\circ$	0.02258893859	0.0216
$\mu_0 = 1.0, \theta = 270^\circ$	0.1110188572	0.1113
$\mu_0 = 0.6, \theta = 0^\circ, 180^\circ$	0.001676516587	0.00165
$\mu_0 = 0.6, \theta = 90^\circ$	0.007209616977	0.0071
$\mu_0 = 0.6, \theta = 270^\circ$	0.02745548914	0.0273
$\mu_0 = 0.2, \theta = 0^\circ, 180^\circ$	0.0001288604229	0.00013
$\mu_0 = 0.2, \theta = 90^\circ$	0.003710427872	0.0037
$\mu_0 = 0.2, \theta = 270^\circ$	0.006989684179	0.0069

Note. Neumann type hard wall boundary conditions are applied. $a = \cosh \mu_0$, $b = \sinh \mu_0$, $\kappa = 0.2$, and incident angle $\alpha = 90^\circ$.

can be obtained in a combination of single- and double-layer formulation of the boundary integral equation [15]. The modifications of the present spectral implementation to other formulations of the boundary integral equation are straightforward.

We also note that the present formulation improves the computational efficiency for both the low and high wave number problems through the reduced size of the resulting algebraic system (19), due to the exponential accuracy achieved in the approximation. Since the cost of direct methods of solving linear system, such as Gauss elimination, increases as $O(N^3)$, some iterative methods may be preferred for the high wave number problems. This, however, is beyond the scope of this paper.

4. CONCLUSIONS

In this paper, a spectral method of solving the boundary integral equation is presented. It is shown that the integral kernels for the Helmholtz equation contain singular terms that have to be removed to achieve the spectral accuracy. Detailed numerical implementation of a Fourier collocation formulation has been given. The non-smoothness of the integration kernels is subtracted out by using a logarithmic function whose Fourier expansion is known. The numerical formulation presented here preserves the spectral accuracy and yields an exponential rate of convergence.

Compared to the boundary element approaches, the spectral boundary integral equation method presented in this paper would yield matrices of much smaller size since the latter requires far fewer points to achieve the same accuracy. This, of course, reduces the complexity and the cost of solving the resultant algebraic system. Since both methods will result in dense matrices, it appears that the spectral formulation is more advantageous for problems with smooth geometries.

ACKNOWLEDGMENTS

The author thanks Drs. J. Webb and D. G. Lasseigne for helpful comments and the suggestions by the referee. This work was supported by the National Aeronautics and Space Administration under NASA Contrast NAS1-19480 while the author was in residence at the Institute for Computer Applications in Science and Engineering, NASA Langley Research Center, Hampton, VA 23665.

REFERENCES

1. C. A. Brebbia and M. S. Ingber, *Boundary Element Technology VII*, Elsevier, Amsterdam, 1992.
2. R. D. Ciskowski and C. A. Brebbia, *Boundary Element Methods in Acoustics*, Comput. Mech. Southampton, 1991.
3. P. C. Waterman, *J. Acoust. Soc. Am.* **45**(6), 1417 (1969).
4. V. K. Varadan and V. V. Varadan, *Acoustic, Electromagnetic and Elastic Wave Scattering—Focus on the T-Matrix Approach* (Pergamon, Elmsford, NY, 1980).
5. W. Toboeman, *J. Acoust. Soc. Am.* **77**(2), 369 (1985).
6. D. Gottlieb and S. Orszag, *Numerical Analysis of Spectral Methods: Theory and Applications* (SIAM, Philadelphia, 1977).
7. C. Canuto, M. Y. Hussaini, A. Quarteroni, and T. A. Zang, *Spectral Methods in Fluid Dynamics* (Springer-Verlag, New York/Berlin, 1988).
8. N. N. Bojarski, *J. Acoust. Soc. Am.* **75**(2), 320 (1984).
9. G. T. Schuster, *J. Acoust. Soc. Am.* **87**(2), 495 (1990).
10. D. Colton and R. Kress, *Integral Equation Methods in Scattering Theory* (Wiley-Interscience, New York, 1983).
11. G. Chen and J. Zhou, *Boundary Element Methods* (Academic Press, New York, 1992).
12. P. Morse and H. Feshbach, *Methods of Theoretical Physics* (McGraw-Hill, New York, 1953).
13. M. Abramowitz and I. A. Stegun, *Handbook of Mathematical Functions* (Dover, New York, 1965).
14. R. Barakat, *J. Acoust. Soc. Am.* **35**(12), 1990 (1963).
15. A. J. Burton and G. F. Miller, *Proc. R. Soc. London A* **323**, 201 (1971).